Supplemental materials

A FVIIIa-mimetic bispecific antibody (Mim8) ameliorates bleeding upon severe vascular challenge in hemophilia A mice

SUPPLEMENTARY METHODS

Emicizumab reference material

Sequence-identical emicizumab was produced in Chinese hamster ovary cells based on the published sequence (WHO Drug Information). Comparison with the commercially available drug (Hemlibra®) using FXIa- and tissue factor (TF)-triggered thrombin generation assays (see below) demonstrated indistinguishable functional properties.

Variant generation

Anti- activated Factor IX (FIXa) and -Factor X (FX) antibodies were expressed using the Expi293 (HEK) system according to manufacturer's instructions (Gibco™; Thermo Fisher Scientific). Antibody variants were prepared with the K409R or F405L DuoBody® mutations and expressed in a plate-based format.[1] Purification of the 4–16 mL supernatants was done using 96-well filterplates (Nunc) packed with 300 µL MabSelect SuRe™ resin (GE Healthcare). Concentrations of purified antibodies were determined from the absorbance at 280 nm using molar extinction coefficients based on sequence. Bispecific antibody (biAb) assembly was performed by mixing the two antibody variants at final concentrations of 4 µM (typically in a reaction volume of 500 µL) in the presence of 75 mM 2-mercaptoethylamine (2-MEA) reducing agent followed by 4-hour incubation at 30°C.[1,2] Removal of 2-MEA after biAb formation was done using spin filter plates with 7-kDa cutoff (Zeba™; Thermo Fisher Scientific). This procedure left 1–2 mM of oxidized 2-MEA in solution as confirmed by nuclear magnetic resonance spectroscopy. Overnight incubation at 4°C allowed for reformation of disulfides to occur. All steps were performed using automated liquid handling (Biomek FXP, BeckmanCoulter). Generation of one-arm (OA) anti-FIXa antibodies followed the protocol above, except that assembly

was performed with a Fc fragment carrying the relevant DuoBody® mutation instead of the anti-FX monoclonal antibody (mAb). Because the assembly efficiency was generally above 90%, biAb and anti-FIXa OA antibodies were screened in high-throughput assays without prior purification.

Production of Mim8 for in-depth characterization followed the protocol above, but with a final isolation of the biAb from residual levels of input antibodies using ion-exchange chromatography.[3] Purity was determined to be >98% and correct identity confirmed by mass spectrometry. Concentration was determined as described above.

Enzyme kinetic analyses

The stimulatory activity of anti-FIXa OA antibodies was measured at a single (initial high throughput screening), or multiple concentrations. At each concentration, a stimulation index was calculated as the ratio of the background subtracted activated FX (FXa) generation in the presence and absence of anti-FIXa OA and with each normalized according to the concentration of FIXa in the assay. FIXa concentrations ranged from 0.15 to 1 nM and were chosen to ensure <15% FX conversion and enough signal for reliable FXa quantification. Full titration curves were fitted to the quadratic binding equation (Eq. 1 and 2 below with anti-FIXa OA replacing biAb)[4] using GraphPad Prism to derive the stimulation at saturation and an apparent equilibrium dissociation constant (K_D) for the anti-FIXa OA-FIXa interaction. The ability of the biAb to assemble with FIXa and FX on the membrane surface was determined from FIXa titrations (0–25 nM) of a limiting concentration of biAb (100 pM) in the presence of 25 nM FX and 417 µM phosphatidylserine (PS):phosphatidylcholine (PC) vesicles. By fitting the rate of FXa generation (r_{FXa}) to Eq. 1 and 2, an apparent K_D for biAb-FIXa-FX-membrane assembly could be estimated.

$$r_{FXa} = a_{FIXa} \cdot \left([FIXa]_t - [FIXa\text{-}biAb]_{eq}\right) + a_{FIXa\cdot biAb} \cdot [FIXa\text{-}biAb]_{eq} \quad \text{Eq. 1}$$

$$[FIXa\text{-}biAb]_{eq} = \frac{([FIXa]_t + [biAb]_t + K_D) - \sqrt{([FIXa]_t + [biAb]_t + K_D)^2 - 4[FIXa]_t[biAb]_t}}{2} \quad \text{Eq. 2}$$

Here, *a* represents the specific activity of the indicated species and the suffixes *t* and *eq* refer to total and equilibrium concentrations, respectively. In order to depict the binding isotherm for the Mim8-FIXa-FX-membrane assembly in Figure 3B, the contribution from free FIXa (represented by

the $a_{FIXa} \cdot \left([FIXa]_t - [\text{FIXa-biAb}]_{eq}\right)$ term in Eq. 1) was subtracted from the measured initial rate of FX activation at each concentration of FIXa. Similarly, the contribution from free FIXa was omitted from the displayed curve fit.

Isothermal titration calorimetry

Binding affinities of Mim8 and the anti-FIXa and anti-FX arms (in mAb format) of biAb46376 for human FIX (BeneFIX®, Pfizer Inc.), FIXa (recombinantly expressed at Novo Nordisk A/S), FX (plasma-derived; HTI), or FXa (plasma-derived; HTI) were measured by isothermal titration calorimetry (ITC) on a PEAQ-ITC calorimeter (Malvern, UK). The experiments were conducted at 25 or 37°C and pH 7.4 in 10 mM HEPES, 150 mM NaCl, 5 mM $CaCl_2$ as indicated in Table S2. The sample cell contained 200 µL of FIX(a) or FX(a) (macromolecule). Antibodies (ligand) was injected via the syringe in a total volume of 40 µL. A thermal equilibration step was followed by a 60-s delay and an initial 0.2-µL injection of antibody, followed by 12–16 injections of 1.5–3 µL of antibody at an interval of 120 s. The stirring speed was maintained at 750 rpm and the reference power was kept constant at 5–10 µcal/s. Raw data were visually inspected and the baseline was adjusted manually. The heat associated with each injection of antibody was integrated and plotted against the molar ratio of ligand to macromolecule. Fitted offset was chosen as the control parameters. The resulting isotherm was fitted to a one-site binding model to obtain the equilibrium dissociation constant (K_D), stoichiometry (N), and enthalpy of interaction (ΔH) using the software provided by the manufacturer.

Epitope mapping

In order to determine residues critical for the interaction between Mim8 and FIX, a set of FIX variants was selected based on the Mim8 anti-FIXa antigen-binding fragment (Fab)/FIXa structure (see Figure 2A and C). C-terminal His-tagged FIX variants were transiently expressed in mammalian cells, purified and characterized with respect to their binding to Mim8 anti-FIXa OA using surface plasmon resonance (SPR) on a Biacore T200 instruments (Biacore AB, Uppsala, Sweden). Measurements were conducted at 25°C, for which anti-His antibody at 25 µg/mL (R&D Systems, catalogue # MAB050) was immobilized on a CM5 sensor chip using standard amine coupling chemistry. FIX variants (25 nM) and wild-type (wt) FIX (BeneFIX®, Pfizer Inc.) were captured at a flow rate of 10 µL/min for 1 min, after which 20 µM (and dilutions thereof) Mim8 anti-FIXa OA was injected at a flow rate of 50

µL/min to measure binding. Dissociation was measured by injecting buffer for 3 min at 50 µL/min. Mim8 anti-FIXa OA and FIX variants were diluted in running buffer (20 mM Tris, 150 mM NaCl, 5 mM $CaCl_2$, 0.05% Tween-20, 10 mg/mL BSA, pH 7.4). Regeneration of the chip was achieved using 10 mM glycine pH 2.0. Binding data were analyzed according to a 1:1 model using BiaEvaluation 4.1 (Biacore AB, Uppsala, Sweden).

Residual binding (%) was calculated according to Eq. 3, where RU_{FIXwt} and RU_{FIXvar} represent capture levels (RU) of wt and variant FIX, respectively; $RU_{Ab:FIXwt}$ and $RU_{Ab:FIXvar}$ the corresponding binding levels (RU) of 20 µM Mim8 anti-FIXa OA.

$$Residual\ binding(\%) = 100\% \cdot \frac{{}^{RU_{Ab:FIXvar}}/_{RU_{FIXvar}}}{{}^{RU_{Ab:FIXwt}}/_{RU_{FIXwt}}} \qquad \text{Eq. 3}$$

Binding of Mim8 to cynomolgus monkey FIX and FX

SPR was performed on a Biacore T200 instrument (GE Healthcare) at 25°C. Anti-FIX (A3B6, Novo Nordisk A/S) and anti-FX (10F2A6, Novo Nordisk A/S) antibodies binding to the Gla domains of FIX and FX, respectively, were immobilized at 25 µg/mL on separate pairs of flow cells on a CM4 sensor chip using standard amine coupling chemistry. One flow cell served as reference, while human FIX (1 and 5 nM, BeneFIX®, Pfizer Inc.), cynomolgus FIX (2.5 and 12.5 nM, Novo Nordisk A/S), human FX (1 and 5 nM, HTI) or cynomolgus FX (2.5 and 12.5 nM, Novo Nordisk A/S) were captured on the other. The binding kinetics of Mim8 anti-FIXa OA (3-fold dilution series starting at 6 µM) to captured FIX or FX was measured in running buffer (10 mM HEPES, 150 mM NaCl, 0.05 % Tween-20, 5 mM $CaCl_2$, 10 mg/mL BSA, pH 7.4). Regeneration of the chip was achieved using the same buffer but with 50 mM EDTA replacing calcium. Recorded sensorgrams were analyzed according to a 1:1 model, and steady-state analysis performed using BiaEvaluation 4.1 (GE Healthcare).

X-ray crystallography

Mim8 anti-FIXa Fab was mixed in a 1:1 molar ratio with human EGR-chloromethylketone (CMK) active-site inhibited des-(Gla-EGF1) FIXa (Cambridge ProteinWorks). The complex was subjected to size exclusion chromatography on a HiLoad 16/60 Superdex 200 pg column (GE Healthcare) run with 20 mM HEPES, pH 7.5, 140 mM NaCl, 1 mM $CaCl_2$ buffer. Complex-containing fractions were pooled

and concentrated to 10.1 mg/mL. Crystals were grown using the microseed matrix screening technique as described elsewhere[5] using sitting-drop vapor diffusion at 18°C. The crystal used was grown from a protein solution of 200 nL 10.1 mg/mL complex in 20 mM HEPES, pH 7.4, 140 mM NaCl, 1 mM $CaCl_2$ mixed with 100 nL seed stock and 300 nL of 2 M ammonium sulphate, 0.1 M HEPES, pH 7.5 as precipitant and incubated over 80 µL precipitant. The seed stock was prepared from crystals of a similar Fab fragment in complex with human EGR-CMK inhibited des-(Gla-EGF1) FIXa.

Anti-FX Fab was mixed in a 1:1 molar ratio with human EGR-CMK active-site-inhibited des-(Gla-EGF1) FXa (Cambridge ProteinWorks) and crystals were grown using the sitting-drop vapor diffusion technique at 18°C. A protein solution of 150 nL 4.7 mg/mL complex in 20 mM Tris, pH 7.4, 50 mM NaCl, and 2.5 mM $CaCl_2$ was mixed with 50 nL of 0.2 M sodium acetate, 0.1 M sodium cacodylate, pH 6.5, 18% (w/v) PEG 8000 as precipitant and incubated over 60 µL precipitant.

The crystals were cryoprotected by addition of 1.5 µL (anti-FIXa Fab/FIXa complex) or 1 µL (anti-FX Fab/FXa complex) of precipitant added 20% of ethylene glycol to the crystallization drop prior to flash cooling in liquid nitrogen. Diffraction data were collected at 100K at the Swiss Light Source at beamlines specified in Table S1. Autoindexing, integration and scaling of the data were performed with programs from the XDS package.[6]

Structures were determined by molecular replacement using Phaser[7] as implemented in Phenix[8] (anti-FIXa Fab/FIXa complex) or Molrep[9] as implemented in the program suite CCP4 (anti-FX Fab/FXa complex).[10] Structures of previously determined Fab fragments in complex with human EGR-CMK-inhibited FIXa or des-(Gla-EGF1) FIXa, respectively, were used as search models. The correct amino acid sequences were built using COOT[11] and structures were then refined using steps of Phenix refinement and manual rebuilding in COOT. Crystal twinning was identified by the Xtriage module from Phenix for the anti-FX Fab/FXa complex and twin refinement was therefore applied throughout refinement. Diffraction data and refinement statistics are summarized in Table S1.

Thrombin generation in human plasma

FXIa-initiated TGT was studied in platelet-poor (PPP) human congenital HA plasma supplemented with phospholipid vesicles (MP-reagent; Thrombinoscope) and optionally 100 U/dL FVIII (turoctocog alfa; Novo Nordisk A/S) to reflect normal conditions. TF-initiated TGT was performed in normal

human platelet-rich plasma (PRP) supplemented with neutralizing anti-FVIII antibody (PAHFVIII-s; HTI). A sample without anti-FVIII antibody was included to represent normal conditions. Thrombin generation was measured at 37°C in a Fluoroskan Ascent plate reader (Thermo Electron Corporation) using reagents, calibrators and software from Thrombinoscope. Data were analyzed using a variable slope four-parameter dose-response model. High-throughput screening of variants in 384-well plates was performed using TF (PPP reagent LOW; Thrombinoscope) and congenital hemophilia A plasma supplemented with phospholipids (Rossix).

Effect studies in hemophilia A mouse injury models

At the end of the bleeding period, total blood loss was determined by spectrophotometric hemoglobin measurement. Plasma levels of biAb and FIX were quantified by a luminescent oxygen channeling assay (LOCI) assays using anti-human immunoglobulin (Ig)G (AFC4249, Nordic Biosite and I3266, Sigma-Aldrich) and anti-FIX antibodies (LS-B7226, LSBio, and FIX-2F24, in-house clone), respectively. FX levels were quantified by a commercial FX ELISA (KSP134, Nordic Biosite). From dose–response studies with biAb, ED_{50}-values were determined by fitting of data to a three-parameter inverse log(dose) response equation with shared plateau values (> 0). Automatic outlier elimination with a 1% ROUT coefficient was applied and sum of squares was weighted by $(\text{blood-loss})^{-1}$.

Pharmacokinetics in cynomolgus monkeys

Sixteen healthy naïve cynomolgus monkeys (*Macaca fascicularis*), 8 females and 8 males (2.3–3.5 kg, aged 2–3 years) were obtained from Bioculture Mauritius Ltd. (Senneville, Mauritius). All animals were purpose-bred and offspring of animals bred in captivity or sourced from self-sustaining colonies ("F1 and F2-generation NHP"). The animals were acclimated to the test facility accommodation for 6 weeks before dosing. Before the dosing, the animals were approved for entry into the experiment based on a satisfactory veterinary examination, clinical observations, body weight profile and clinical pathology investigations. The animals were allocated a cage in groups of up to 4. After allocation to dose groups, the animals were identified by a subcutaneously implanted electronic identification chip.

To reduce the number of animals used in the study, a within-individual dose-escalation design was chosen as described elsewhere.[12] The intravenous group received two doses via the tail vein: the

first dose (Group 1: 0.3 mg/kg, Group 2: 1 mg/kg) on Day 0 and the second dose (Group 1: 3 mg/kg, Group 2: 6 mg/kg) on Day 7. The subcutaneous group received one dose (1 mg/kg) in the back on Day 0 only. For each timepoint (see Figure 6), 1.6 mL blood per animal were collected from the femoral vein and diluted 1:10 in 3.2% (w/v) citrate before plasma was prepared. Plasma concentrations of Mim8 were measured by a fit-for-purpose qualified LOCI assay using a polyclonal antibody against human IgG (Biosite, cat. no. AFC4249) and an in-house monoclonal antibody (NNC1212-0000-0421) against human IgG. FIX plasma concentration was quantified by LOCI as described for detection in mouse plasma. Plasma FX was quantified by a commercial FX ELISA (Zymutest RK033A, Hyphen Biomed).

Calculation of pharmacokinetic parameters and descriptive statistics were performed using Phoenix 64 (v. 7.0, Pharsight Inc.) and individual concentration–time values obtained from each animal.

SUPPLEMENTARY FIGURES

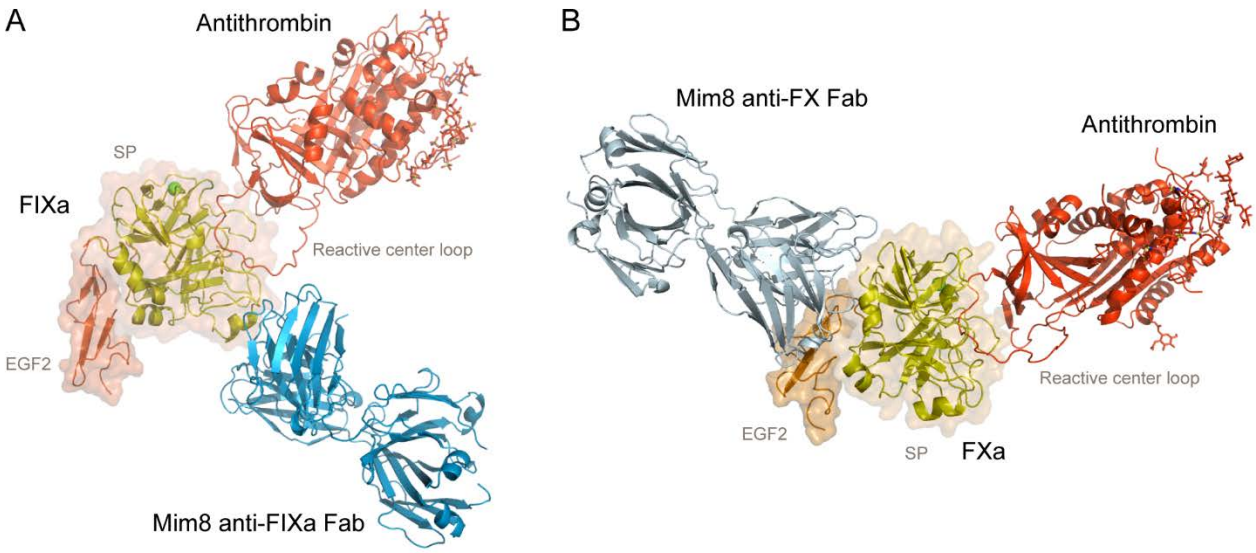

Figure S1. Structure model of FIXa and FXa in complex with antithrombin and Mim8 Fab fragments. Crystal structures of the Mim8 anti-FIXa (A) and anti-FX (B) Fab fragments in complex with EGR-CMK active-site-inhibited des-(gla-EGF1) FIXa and FXa, respectively, docked in published crystal structure of FIXa-antithrombin complex (PDB ID: 3KCG)[13] and FXa -antithrombin complex (PDB ID: 2GD4),[14] respectively.

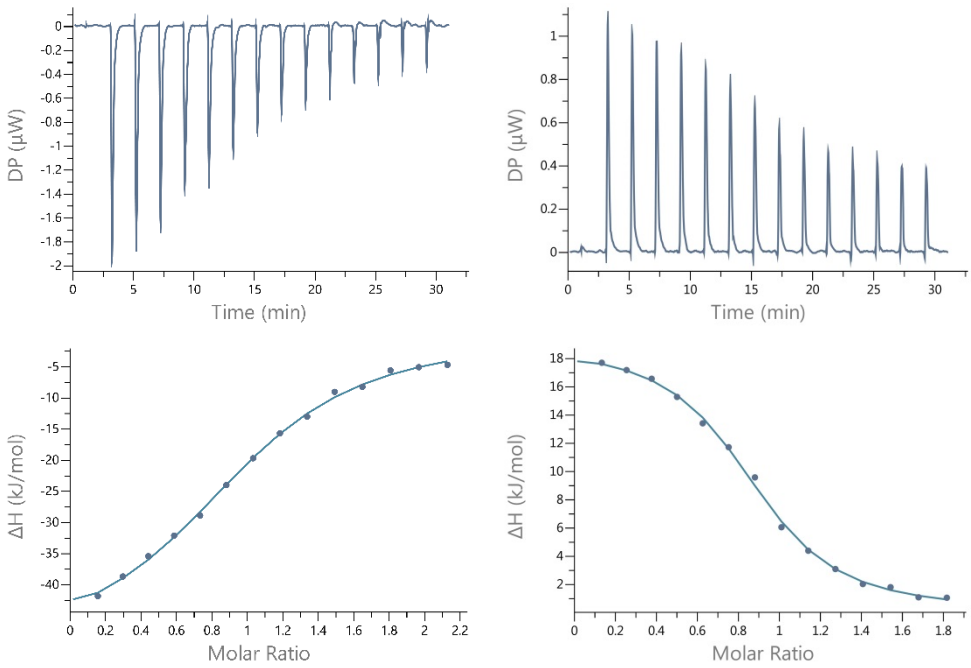

Figure S2. Binding isotherms for the interaction of FIX or FX with Mim8 as measured by ITC. FIX binding (left panel) to Mim8 is characterized by strong exothermic binding signal (–54 kJ/mole) and a K_D of 4.7 ± 0.7 µM. FX binding (right panel) is characterized by a weak endothermic binding signal (12.8 kJ/mole) and a K_D of 1.5 ± 0.4 µM. Titrations were performed at pH 7.4 and 37°C.

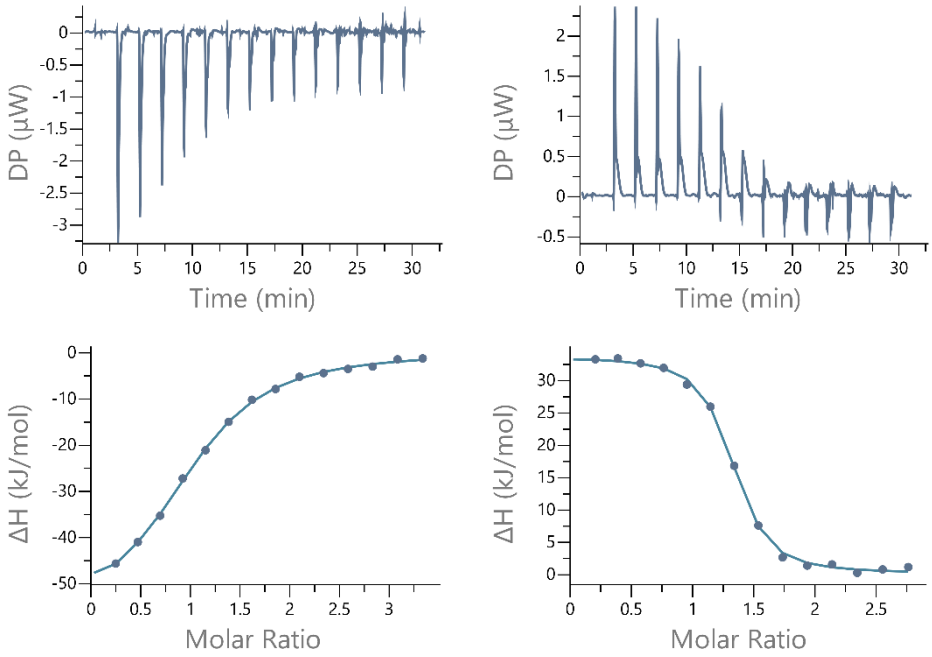

Figure S3. Binding isotherms for the interaction of FIXa or FXa with Mim8 as measured by ITC. FIXa binding (left panel) to Mim8 is characterized by strong exothermic binding signal (–53.9 kJ/mole) and a K_D of 2.3 ± 0.3 µM at 37°C and pH 7.4. FXa binding (right panel) to Mim8 was performed at 25°C and pH 7.4 and characterized by an endothermic binding signal (33.6 kJ/mole) and a K_D of 0.3 ± 0.1 µM.

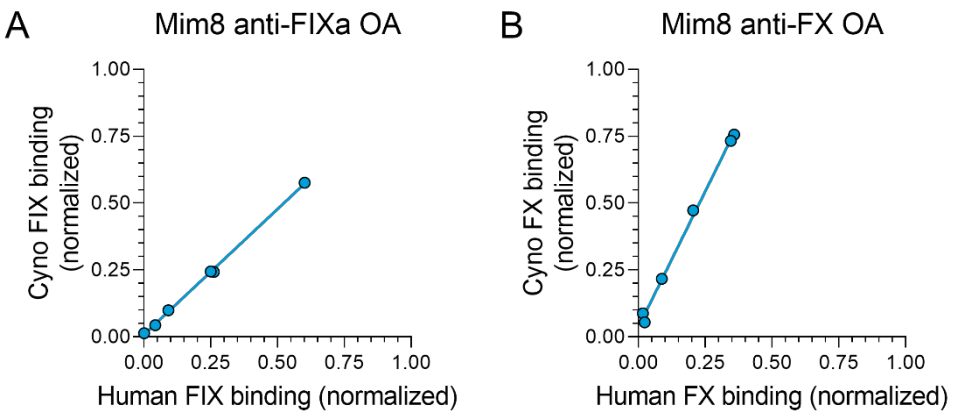

Figure S4. Binding of Mim8 anti-FIXa and anti-FX OA antibodies to human and cynomolgus monkey FIX or FX. (A) Binding levels of Mim8 anti-FIXa OA to human or cynomolgus monkey (cyno) FIX were measured at steady state using SPR as described in Supplementary Methods. To account for variations in FIX capture, each OA antibody binding response was normalized according to the initial capture level of FIX. With a slope of 0.94 for the normalized binding of Mim8 anti-FIXa OA to cynomolgus monkey versus human FIX, it could be concluded that the Mim8 anti-FIXa arm recognizes FIX from the two species equally well. (B) A similar analysis of Mim8 anti-FX OA binding to cynomolgus monkey and human FX provided a slope of 2.03, demonstrating a slightly improved binding of the Mim8 anti-FX arm to cynomolgus monkey FX.

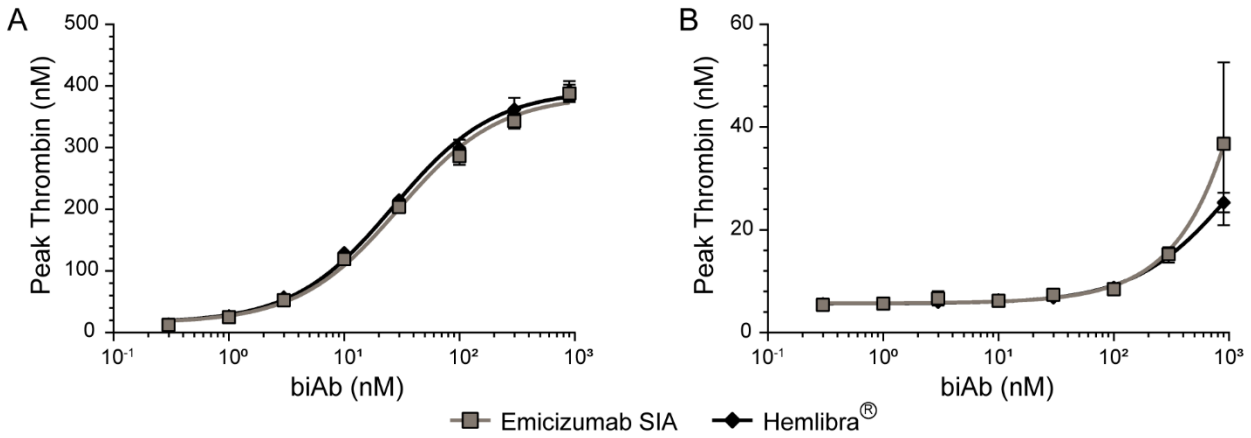

Figure S5: Activity of emicizumab SIA and commercially available Hemlibra® in plasma-based assays. A) Concentration-dependent peak thrombin generation of emicizumab SIA and Hemlibra® in TGT using FVIII deficient plasma triggered with 8.3 mU/mL human FXIa. B) Concentration-dependent peak thrombin generation of emicizumab SIA and Hemlibra® in TGT using FVIII-deficient plasma triggered with 1 pM TF.

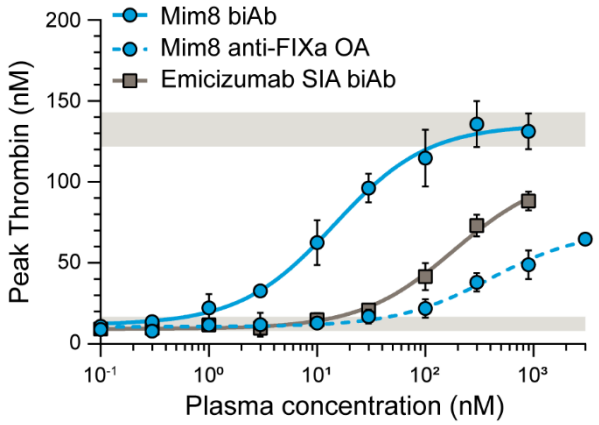

Figure S6: Activity of Mim8 anti-FIXa OA in plasma-based assay. Concentration-dependent thrombin generation of Mim8 anti-FIXa OA compared with Mim8 biAb and emicizumab SIA biAb in platelet-rich plasma triggered with 1 pM TF.

SUPPLEMENTARY TABLES

Table S1. Diffraction data and refinement statistics for the Mim8 anti-FIXa Fab and anti-FX Fab complexes with human EGR-CMK active-site-inhibited des-(Gla-EGF1) FIXa and des-(gla-EGF2) FXa, respectively. Statistics for the highest-resolution shell are shown in parentheses.

Complex	Mim8 anti-FIXa Fab/EGR-CMK-inhibited des-(Gla-EGF1)-FIXa	Mim8 anti-FX Fab/EGR-CMK-inhibited des-(Gla-EGF1)-FXa
Beamline (SLS)	X10SA	X06DA
Detector	Pilatus3 6M (Dectris)	Pilatus2M (Dectris)
Wavelength (Å)	1.000	1.000
Resolution range (Å)	48.51–3.11 (3.221–3.11)	44.12–2.6 (2.693–2.6)
Space group	P 4_122	P2_1
Unit cell (Å, deg)	97.03 97.03 254.51 90 90 90	63.13 105.25 145.78 90 89.995 90
Total reflections	295,554 (29,569)	302,807 (30,703)
Unique reflections	22,733 (2211)	58,767 (5896)
Multiplicity	13.0 (13.4)	5.2 (5.2)
Completeness (%)	99.87 (99.86)	99.90 (99.97)
Mean I/sigma (I)	4.32 (0.99)	12.31 (1.56)
Wilson B-factor (Å^2)	50.59	50.13
R-merge	0.6915 (2.526)	0.1209 (1.024)
R-meas	0.7198 (2.627)	0.1346 (1.138)
R-pim	0.1983 (0.7129)	0.05869 (0.4933)
CC1/2	0.959 (0.492)	0.996 (0.523)
CC*	0.989 (0.812)	0.999 (0.829)
Reflections used in refinement	22714 (2208)	58761 (5896)
Reflections used for R-free	547 (52)	1999 (202)
R-work	0.2280 (0.3369)	0.2033 (0.3027)
R-free	0.2844 (0.3981)	0.2623 (0.3140)
CC (work)	0.937 (0.742)	0.857 (0.463)
CC (free)	0.917 (0.608)	0.788 (0.347)

Number of non-hydrogen atoms	5700	11,641
Macromolecules	5589	11,145
Ligands	111	52
Solvent	–	444
Protein residues	726	1447
RMS (bonds) (Å)	0.012	0.011
RMS (angles) (deg)	1.49	1.70
Ramachandran favored (%)	96.94	95.74
Ramachandran allowed (%)	2.79	3.70
Ramachandran outliers (%)	0.28	0.56
Rotamer outliers (%)	0.96	0.32
Clashscore	4.21	22.55
Average B-factor (Å^2)	42.89	46.64
Macromolecules	42.65	46.94
Ligands	54.70	46.66
Solvent	–	39.14
Twin refinement (operator, fraction)	–	h,-k,-l 0.46
Protein Data Bank Id	7AHV	7AHU

Table S2. **Summary of results from binding studies of biAb46376 and Mim8 to human FIX(a) and FX(a) using ITC.** The following abbreviations are used: n (number of experiments), N (binding stoichiometry or number of binding sites), K_D (estimated mean equilibrium binding constant and error of the fit), ΔH = (enthalpic contribution of the interaction), and -TΔS (entropic contribution of the interaction). See corresponding Figure S2 and S3.

Antibody	**Ligand**	**Temp (˚C)**	**n**	**N**	**K_D**	**ΔH (kJ/mol)**	**-TΔS (kJ/mol)**
Anti-FIXa mAb from biAb46376	Human FIXa	37	2	0.44	1.7 ± 0.5 nM	–271	218
Anti-FX mAb from biAb46376	Human FX	37	1	0.46	101 ± 12 nM	–39.2	–2.4

Mim8	Human FX	37	4	1.08	1.5 ± 0.4 µM	12.8	–47.7
Mim8	Human FXa	25	3	1.27	0.3 ± 0.1 µM	33.6	–70.6
Mim8	Human FIX	37	2	0.99	4.7 ± 0.7 µM	-54.0	22.3
Mim8	Human FIXa	37	3	0.89	2.3 ± 0.3 µM	-53.9	20.4

Table S3. Summary of pharmacokinetic-parameter estimates of Mim8 in cynomolgus monkey after intravenous dosing on day 7 (168 hours) and subcutaneous dosing on day 0. Results are shown as mean ± standard deviation. The following abbreviations are used: time to maximum plasma concentration (Tmax), maximum plasma concentration (Cmax), dose-normalized area under the curve (AUC/Dose), half-life ($t_{½}$), intravenous clearance (CL), subcutaneous clearance (CL/F), subcutaneous bioavailability (F) intravenous (IV), subcutaneous (SC), not applicable (N/A).

Group	Route	Dose (mg/kg)	Tmax (hr)	Cmax (nmol/L)	AUC/Dose (hr*kg/L)	$t_{½}$ (hr)	CL or CL/F (mL/hr/kg)	F (%)
1	IV	3.0	168	559 ± 67	(6.5 ± 1.4) $\times 10^3$	326 ± 97	0.16 ± 0.03	N/A
2	IV	6.0	168	(1.14 ± 0.07) $\times 10^3$	(6.8 ± 1.6) $\times 10^3$	283 ± 93	0.15 ± 0.03	N/A
3	SC	1.0	96.0	84 ± 17	(6.1 ± 1.5) $\times 10^3$	340 ± 70	0.17 ± 0.04	97.3 ± 8.3

SUPPLEMENTARY REFERENCES

1. Labrijn AF, Meesters JI, de Goeij BE, et al. Efficient generation of stable bispecific IgG1 by controlled Fab-arm exchange. *Proc Natl Acad Sci U S A*. 2013;110(13):5145-5150.
2. Labrijn AF, Meesters JI, Priem P, et al. Controlled Fab-arm exchange for the generation of stable bispecific IgG1. *Nat Protoc*. 2014;9(10):2450-2463.
3. Gramer MJ, van den Bremer ET, van Kampen MD, et al. Production of stable bispecific IgG1 by controlled Fab-arm exchange: scalability from bench to large-scale manufacturing by application of standard approaches. *MAbs*. 2013;5(6):962-973.
4. Krishnaswamy S. The interaction of human factor VIIa with tissue factor. *J Biol Chem*. 1992;267(33):23696-23706.
5. D'Arcy A, Bergfors T, Cowan-Jacob SW, Marsh M. Microseed matrix screening for optimization in protein crystallization: what have we learned? *Acta Crystallogr F Struct Biol Commun*. 2014;70(Pt 9):1117-1126.
6. Kabsch W. XDS. *Acta Crystallogr D Biol Crystallogr*. 2010;66(Pt 2):125-132.
7. McCoy AJ, Grosse-Kunstleve RW, Adams PD, Winn MD, Storoni LC, Read RJ. Phaser crystallographic software. *J Appl Crystallogr*. 2007;40(Pt 4):658-674.
8. Adams PD, Afonine PV, Bunkoczi G, et al. PHENIX: a comprehensive Python-based system for macromolecular structure solution. *Acta Crystallogr D Biol Crystallogr*. 2010;66(Pt 2):213-221.
9. Vagin A, Teplyakov A. MOLREP: an automated program for molecular replacement. *J Appl Crystallogr*. 1997;30:1022-1025.
10. Winn MD, Ballard CC, Cowtan KD, et al. Overview of the CCP4 suite and current developments. *Acta Crystallographica Section D*. 2011;67(4):235-242.
11. Emsley P, Lohkamp B, Scott WG, Cowtan K. Features and development of Coot. *Acta Crystallogr D Biol Crystallogr*. 2010;66(Pt 4):486-501.
12. Patnaik A, Kang SP, Rasco D, et al. Phase I study of pembrolizumab (MK-3475; anti-PD-1 monoclonal antibody) in patients with advanced solid tumors. *Clin Cancer Res*. 2015;21(19):4286-4293.
13. Johnson DJD, Langdown J, Huntington JA. Molecular basis of factor IXa recognition by heparin-activated antithrombin revealed by a 1.7-Å structure of the ternary complex. *Proc Natal Acad Sci*. 2010;107(2):645-650.
14. Johnson DJD, Li W, Adams TE, Huntington JA. Antithrombin–S195A factor Xa–heparin structure reveals the allosteric mechanism of antithrombin activation. *EMBO J*. 2006;25:2029-2037.